Supplement of Clim. Past, 17, 507–528, 2021
https://doi.org/10.5194/cp-17-507-2021-supplement

Climate of the Past
Open Access
EGU

Supplement of

Lower oceanic δ^{13}C during the last interglacial period compared to the Holocene

Shannon A. Bengtson et al.

Correspondence to: Shannon A. Bengtson (s.bengtson@unsw.edu.au)

Text S1

Though long term imbalances between weathering and burial of carbon are the likely cause for the δ^{13}C LIG-Holocene anomaly (Jeltsch-Thömmes et al., 2019; Jeltsch-Thömmes and Joos, 2020), an alternate explanation may be that there was a change in the carbon stored in the terrestrial biosphere.

Past studies have estimated terrestrial carbon by considering conservation equations for total carbon and ^{13}C during other periods (e.g. Menviel et al., 2017; Peterson et al., 2014), however there is no published proxy-based global estimate for the LIG terrestrial carbon. Here, we present mass balances of the total carbon and ^{13}C for the LIG and the Holocene. We use our estimation of a mean oceanic δ^{13}C anomaly of -0.2 ‰ during the LIG than the Holocene to calculate the change in terrestrial carbon. These equations assume that the total mass of carbon and the mass of ^{13}C within the atmosphere-land-ocean system did not change between the LIG and the Holocene and that it was merely redistributed between these three reservoirs, thereby excluding exchanges with the lithosphere. The mass balance for ^{13}C during the LIG and the Holocene can be expressed as:

$$\begin{aligned} &\int\int\int \delta^{13}\mathrm{C_{AL}C_{AL}dV} + \int\int\int \delta^{13}\mathrm{C_{OL}C_{OL}dV} + \int\int \delta^{13}\mathrm{C_{TL}C_{TL}dA} \\ &= \\ &\int\int\int \delta^{13}\mathrm{C_{AH}C_{AH}dV} + \int\int\int \delta^{13}\mathrm{C_{OH}C_{OH}dV} + \int\int \delta^{13}\mathrm{C_{TH}C_{TH}dA}, \end{aligned} \tag{1}$$

and for the total amount of carbon:

$$\begin{aligned} &\int\int\int \mathrm{C_{AL}dV} + \int\int\int \mathrm{C_{OL}dV} + \int\int \mathrm{C_{TL}dA} \\ &= \\ &\int\int\int \mathrm{C_{AH}dV} + \int\int\int \mathrm{C_{OH}dV} + \int\int \mathrm{C_{TH}dA}, \end{aligned} \tag{2}$$

where for $\delta^{13}\mathrm{C}_{location,period}$ (‰) and $\mathrm{C}_{location,period}$ (Gt C) period is L (last interglacial period) or H (Holocene), and location is A (atmosphere), O (ocean), or T (terrestrial biosphere). V and A in the integrals are volume and area respectively.

Using these equations, we estimate the total amount of terrestrial carbon based on CO_2 and $\delta^{13}CO_2$ from ice cores and our estimate of the mean ocean $\delta^{13}C$ anomaly of 0.2 ‰ in the ocean.

We estimate the total terrestrial carbon at 2,320 Gt C during the Holocene. This is 50 Gt C less than the pre-industrial estimate of 2,370 Gt C from Köhler and Fischer (2004) and Ciais et al. (2012) and accounts for the difference between PI and the Holocene based on ice core estimates (Elsig et al., 2009a). The Holocene ocean carbon reservoir is taken at 36,830±170 Gt C, which comes from the PI estimate from Ciais et al. (2012). We test the upper and lower limit of this estimate. We also test a scenario where we account for the difference in the ocean carbon reservoir between PI and the Holocene by assuming 115 Gt C less oceanic carbon than the minimum estimate of the Holocene (36,545 Gt C). We obtain 115 Gt C using a mass balance of the difference between the Holocene and PI in atmospheric $\delta^{13}CO_2$ from Elsig et al. (2009b), the aforementioned terrestrial carbon difference of 50 Gt C, and loss of carbon due to sedimentation simulated in Menviel and Joos (2012).

In line with previous studies (e.g. Menviel et al., 2017), we assume that the atmospheric $\delta^{13}CO_2$ and CO_2 is homogeneous for both time periods. We estimate the atmospheric carbon content based on Eggleston et al. (2016) and Schneider et al. (2013) for the LIG (125–120 ka BP) and Holocene (7–2 ka BP), respectively, based on EPICA Dome C and Talos Dome ice core data (Fig. 1d). We estimate LIG and Holocene CO_2 from the stacks found in Köhler et al. (2017) (Fig. 1a).

We use an average terrestrial carbon fractionation of -24.3 ‰ based on PI estimates and consider it to be unchanged from the Holocene. Since the average $\delta^{13}C$ of the terrestrial biosphere depends on the ratio of different plant species, particularly the ratio of C3 to C4 plants, plant species distributions during both the LIG and the Holocene are required for an accurate estimate. However, while the available literature suggests significant vegetation changes at the LIG compared to the Holocene (e.g. Sánchez Goñi et al., 2005), there is no available global reconstruction of plant type distributions based on proxy data (Otto-Bliesner et al., 2016). Without a reliable estimate of average $\delta^{13}C$ for the terrestrial biosphere during the LIG, we need to estimate a reasonable range of variation. The Last Glacial Maximum (LGM) mean terrestrial carbon value has been estimated as -23.3 ‰, ∼1 ‰ higher than during the Holocene (Joos et al., 2004; Ciais et al., 2012). Since vegetation distributions and climatic differences that affect $\delta^{13}C$ were probably smaller between the LIG and the Holocene than between the LGM and the Holocene, the variation in mean terrestrial $\delta^{13}C$ should be less. So, we base our LIG $\delta^{13}C$ estimate on the PI value but we consider 1 ‰ as the maximum variability we could expect on this estimate. We therefore test a mean terrestrial $\delta^{13}C$ of -24.3±0.5 ‰ for the LIG in our calculations.

To our knowledge, total oceanic carbon has not been estimated for the LIG in any prior studies. Assuming that the total carbon content has remained the same across the two time periods, we use the two equations (Equations 1 and 2) simultaneously by substituting the unknown global ocean carbon content

for the LIG. After this, we calculate the global terrestrial carbon content as per Equation 3 using the estimates of δ^{13}C of the ocean for the LIG and the Holocene from this study.

$$C_{\mathrm{TL}} = \frac{C_{\mathrm{AH}}\delta^{13}C_{\mathrm{AH}} + C_{\mathrm{OH}}\delta^{13}C_{\mathrm{OH}} + C_{\mathrm{TH}}\delta^{13}C_{\mathrm{TH}} - C_{\mathrm{AL}}\delta^{13}C_{\mathrm{AL}} - \delta^{13}C_{\mathrm{OL}}(C_{\mathrm{AH}} + C_{\mathrm{OH}} + C_{\mathrm{TH}} - C_{\mathrm{AL}})}{\delta^{13}C_{\mathrm{TL}} - \delta^{13}C_{\mathrm{OL}}} \tag{3}$$

We obtain $\sim$310$\pm$44 Gt C less terrestrial carbon during the LIG compared to the Holocene following the scenarios detailed above (Table S1). The terrestrial carbon storage value is most sensitive to the uncertainty in the LIG mean terrestrial δ^{13}C, while the results are relatively robust to uncertainties in the marine carbon reservoirs. Furthermore, using this estimate with Equation 2 we estimate a global ocean carbon reservoir to be 252-338 Gt C greater during the LIG compared to the Holocene.

Even though these calculations suggest that the carbon stored in soils at the LIG was lower than during the Holocene, our mass balance approach contains significant uncertainties due to the closed system assumption. We therefore suggest that imbalances in the burial and weathering fluxes of carbon explain the 0.2 ‰ LIG-Holocene anomaly.

Table S1: Global mass balance sensitivity analysis variable inputs and calculated results. Variable estimates: pre-industrial oceanic carbon (C_{OP}, Gt C) and $\delta^{13}C$ for the last interglacial terrestrial biosphere ($\delta^{13}C_{TL}$, ‰). Calculated results: last interglacial oceanic carbon (C_{OL}, Gt C), last interglacial terrestrial carbon (C_{TL}, Gt C) and the change in terrestrial carbon from LIG to pre-industrial (ΔC_T, ‰).

C_{OP}	$\delta^{13}C_{TL}$	C_{OL}	C_{TL}	ΔC_T
36545	-24.8	36879	1999	-350
36545	-24.3	36839	2040	-309
36545	-23.8	36796	2083	-266
36545	-24.8	36879	1999	-350
36545	-24.3	36839	2040	-309
36545	-23.8	36796	2083	-266
36660	-24.8	36995	1999	-350
36660	-24.3	36955	2039	-310
36660	-23.8	36912	2082	-267
36660	-24.8	36995	1999	-350
36660	-24.3	36955	2039	-310
36660	-23.8	36912	2082	-267
36830	-24.8	37167	1997	-352
36830	-24.3	37126	2038	-311
36830	-23.8	37083	2080	-269
36830	-24.8	37167	1997	-352
36830	-24.3	37126	2038	-311
36830	-23.8	37083	2080	-269
37000	-24.8	37338	1996	-353
37000	-24.3	37297	2037	-312
37000	-23.8	37255	2079	-270
37000	-24.8	37338	1996	-353
37000	-24.3	37297	2037	-312
37000	-23.8	37255	2079	-270

Supporting Figures

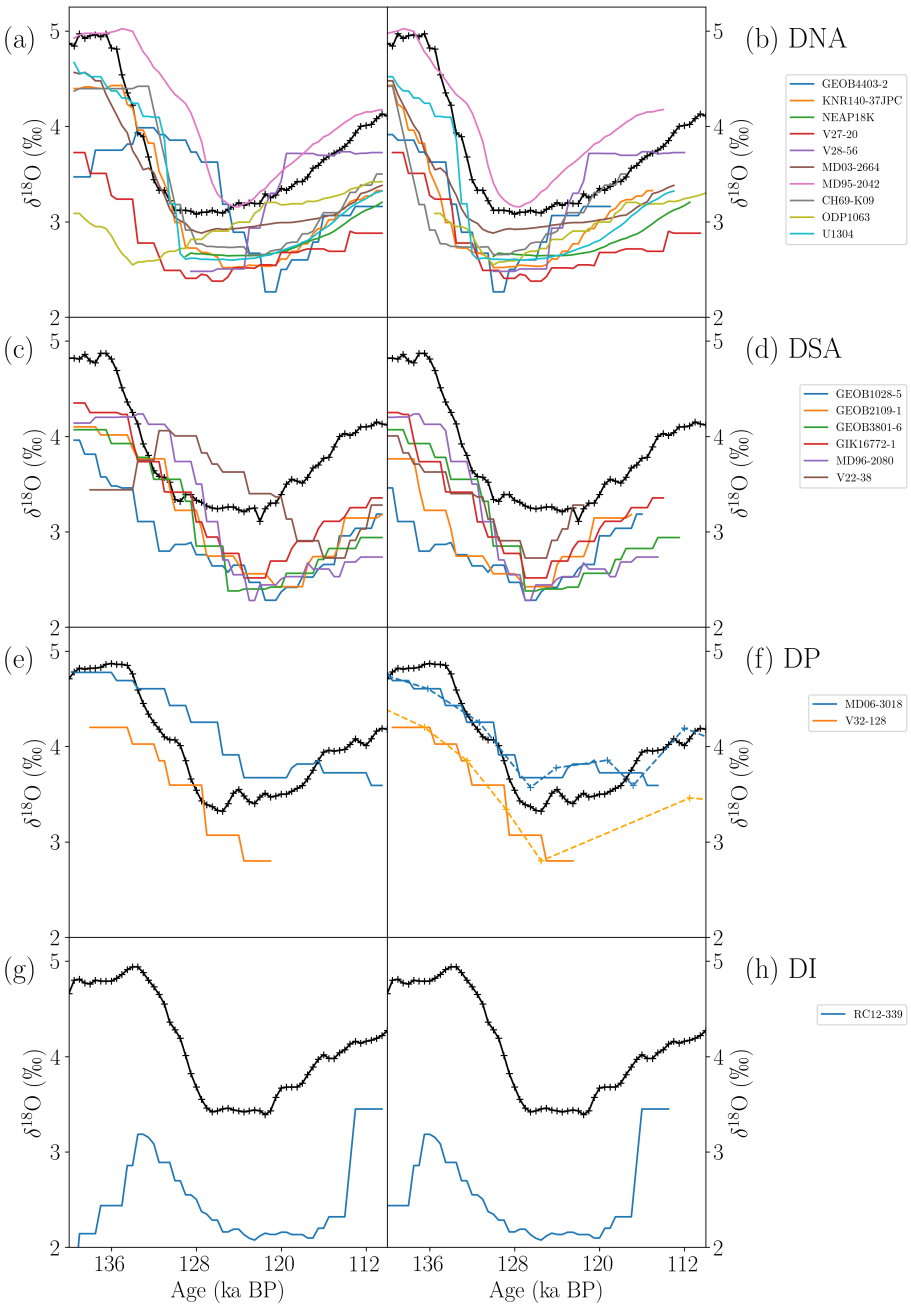

Figure S1: Benthic δ^{18}O from cores which had not been previously aligned to LS16: before (panels a, c, e, g) and after (panels b, d, f, h) adjustments applied in this study to align the δ^{18}O minimum from each core to the nearest LS16 stack δ^{18}O minimum (black lines, Lisiecki and Stern (2016)) covering the LIG. Regions: DNA: deep north Atlantic, DSA: deep south Atlantic, DP: deep Pacific, DI: deep Indian.

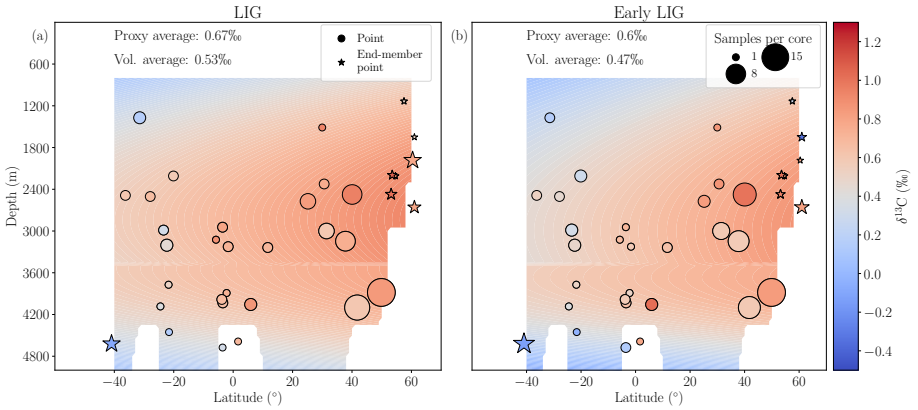

Figure S2: Reconstructed Atlantic δ^{13}C (‰) meridional section during the LIG (125–120 ka BP) and Early LIG (128–123 ka BP). The circular points represent the proxy data which shows the average δ^{13}C with colour and the number of points per core with size. The stars represent the proxy data which make up the end-members. Background shading shows the reconstructed δ^{13}C using a quadratic statistical regression of the proxy data following the method described in Bengtson et al. (2019).

References

Bengtson, S. A., Meissner, K. J., Menviel, L., A. Sisson, S., and Wilkin, J.: Evaluating the extent of North Atlantic Deep Water and the mean Atlantic δ^{13}C from statistical reconstructions, Paleoceanography and Paleoclimatology, https://doi.org/10.1029/2019PA003589, 2019.

Ciais, P., Tagliabue, A., Cuntz, M., Bopp, L., Scholze, M., Hoffmann, G., Lourantou, A., Harrison, S. P., Prentice, I. C., Kelley, D. I., Koven, C., and Piao, S. L.: Large inert carbon pool in the terrestrial biosphere during the Last Glacial Maximum, Nature Geoscience, 5, 74–79, https://doi.org/10.1038/ngeo1324, URL `https://www.nature.com/articles/ngeo1324`, 2012.

Eggleston, S., Schmitt, J., Bereiter, B., Schneider, R., and Fischer, H.: CO_2 concentration and stable isotope ratios of three Antarctic ice cores covering the period from 149.4 - 1.5 kyr before 1950, PANGAEA, https://doi.org/10.1594/PANGAEA.859181, URL `https://doi.org/10.1594/PANGAEA.859181`, 2016.

Elsig, J., Schmitt, J., Leuenberger, D., Schneider, R., Eyer, M., Leuenberger, M., Joos, F., Fischer, H., and Stocker, T. F.: Carbon isotopic record of CO_2 from the Holocene of the Dome C

ice core, PANGAEA, https://doi.org/10.1594/PANGAEA.728699, URL https://doi.org/10.1594/PANGAEA.728699, 2009a.

Elsig, J., Schmitt, J., Leuenberger, D., Schneider, R., Eyer, M., Leuenberger, M., Joos, F., Fischer, H., and Stocker, T. F.: Stable isotope constraints on Holocene carbon cycle changes from an Antarctic ice core, Nature, 461, 507–510, https://doi.org/10.1038/nature08393, URL https://www.nature.com/articles/nature08393, 2009b.

Jeltsch-Thömmes, A. and Joos, F.: The response to pulse-like perturbations in atmospheric carbon and carbon isotopes, Climate of the Past Discussions, pp. 1–36, https://doi.org/https://doi.org/10.5194/cp-2019-107, URL https://www.clim-past-discuss.net/cp-2019-107/, 2020.

Jeltsch-Thömmes, A., Battaglia, G., Cartapanis, O., Jaccard, S. L., and Joos, F.: Low terrestrial carbon storage at the Last Glacial Maximum: constraints from multi-proxy data, Climate of the Past, 15, 849–879, https://doi.org/z‘, URL https://www.clim-past.net/15/849/2019/, 2019.

Joos, F., Gerber, S., Prentice, I. C., Otto-Bliesner, B. L., and Valdes, P. J.: Transient simulations of Holocene atmospheric carbon dioxide and terrestrial carbon since the Last Glacial Maximum, Global Biogeochemical Cycles, 18, https://doi.org/10.1029/2003GB002156, URL https://agupubs.onlinelibrary.wiley.com/doi/abs/10.1029/2003GB002156, 2004.

Köhler, P. and Fischer, H.: Simulating changes in the terrestrial biosphere during the last glacial/interglacial transition, Global and Planetary Change, 43, 33–55, https://doi.org/10.1016/j.gloplacha.2004.02.005, URL http://www.sciencedirect.com/science/article/pii/S0921818104000542, 2004.

Köhler, P., Nehrbass-Ahles, C., Schmitt, J., Stocker, T. F., and Fischer, H.: Continuous record of the atmospheric greenhouse gas carbon dioxide (CO_2), raw data, PANGAEA, https://doi.org/10.1594/PANGAEA.871265, URL https://doi.pangaea.de/10.1594/PANGAEA.871265, 2017.

Lisiecki, L. E. and Stern, J. V.: Regional and global benthic δ^{18}O stacks for the last glacial cycle, Paleoceanography, 31, 2016PA003 002, https://doi.org/10.1002/2016PA003002, URL http://onlinelibrary.wiley.com/doi/10.1002/2016PA003002/abstract, 2016.

Menviel, L. and Joos, F.: Toward explaining the Holocene carbon dioxide and carbon isotope records: Results from transient ocean carbon cycle-climate simulations, Paleoceanography, 27, https://doi.org/10.1029/2011PA002224, URL https://agupubs.onlinelibrary.wiley.com/doi/abs/10.1029/2011PA002224, 2012.

Menviel, L., Yu, J., Joos, F., Mouchet, A., Meissner, K. J., and England, M. H.: Poorly ventilated deep ocean at the Last Glacial Maximum inferred from carbon isotopes: A data-model comparison study, Paleoceanography, 32, 2–17, https://doi.org/10.1002/2016PA003024, URL https://agupubs.onlinelibrary.wiley.com/doi/abs/10.1002/2016PA003024, 2017.

Otto-Bliesner, B. L., Braconnot, P., Harrison, S. P., Lunt, D. J., Abe-Ouchi, A., Albani, S., Bartlein, P. J., Capron, E., Carlson, A. E., Dutton, A., Fischer, H., Goelzer, H., Govin, A., Haywood, A., Joos, F., Legrande, A. N., Lipscomb, W. H., Lohmann, G., Mahowald, N., Nehrbass-Ahles, C., Pausata, F. S.-R., Peterschmitt, J.-Y., Phipps, S., and Renssen, H.: The PMIP4 contribution to CMIP6 - Part 2: Two Interglacials, Scientific Objective and Experimental Design for Holocene and Last Interglacial Simulations, Geosci. Model Dev. Discuss., 2016, 1–36, https://doi.org/10.5194/gmd-2016-279, URL http://www.geosci-model-dev-discuss.net/gmd-2016-279/, 2016.

Peterson, C. D., Lisiecki, L. E., and Stern, J. V.: Deglacial whole-ocean δ^{13}C change estimated from 480 benthic foraminiferal records, Paleoceanography, 29, 549–563, https://doi.org/10.1002/2013PA002552, URL https://agupubs.onlinelibrary.wiley.com/doi/abs/10.1002/2013PA002552, 2014.

Sánchez Goñi, M. F., Loutre, M. F., Crucifix, M., Peyron, O., Santos, L., Duprat, J., Malaizé, B., Turon, J. L., and Peypouquet, J. P.: Increasing vegetation and climate gradient in Western Europe over the Last Glacial Inception (122–110 ka): data-model comparison, Earth and Planetary Science Letters, 231, 111–130, https://doi.org/10.1016/j.epsl.2004.12.010, URL http://www.sciencedirect.com/science/article/pii/S0012821X04007162, 2005.

Schneider, R., Schmitt, J., Köhler, P., Joos, F., and Fischer, H.: A reconstruction of atmospheric carbon dioxide and its stable carbon isotopic composition from the penultimate glacial maximum to the last glacial inception, Climate of the Past, 9, 2507–2523, https://doi.org/10.5194/cp-9-2507-2013, URL http://www.clim-past.net/9/2507/2013/, 2013.